Absolute partial cross sections for electron-impact ionization of CH_4 from threshold to 1000 eV

H. C. Straub, D. Lin, B. G. Lindsay, K. A. Smith, and R. F. Stebbings
Department of Space Physics and Astronomy, Department of Physics, and Rice Quantum Institute, Rice University, 6100 Main Street, Houston, Texas 77005-1892

(Received 28 October 1996; accepted 11 December 1996)

Absolute partial cross sections for the production of CH_4^+, CH_3^+, CH_2^+, CH^+, C^+, H_2^+, and H^+ from electron-impact ionization of CH_4 are reported for electron energies from threshold to 1000 eV. The product ions are mass analyzed using a time-of-flight mass spectrometer and detected with a position-sensitive detector whose output demonstrates that all product ions are completely collected. The overall uncertainty in the absolute cross section values is $\pm 3.5\%$ for singly charged parent ions and is slightly greater for fragment ions. Although previous measurements are generally found to agree well with the present results for CH_4^+ and CH_3^+, almost all previous work for the remaining fragment ions lies lower than the present results and in the case of H^+ is lower by approximately a factor of 4. © *1997 American Institute of Physics.* [S0021-9606(97)01511-0]

I. INTRODUCTION

Cross sections for electron-impact ionization of CH_4 are of importance for understanding the physics and chemistry of planetary atmospheres and plasma processing. The first total cross section measurements for CH_4 were made by Hughes and Klein.[1] Absolute total cross section measurements have since been made by Rapp and Englander-Golden[2] and Schram *et al.*[3] Relative total cross section measurements made by Tozer,[4] Winters,[5] and Chatham *et al.*[6] were placed on an absolute scale by normalizing to a previously measured absolute total cross section. Rapp, Englander-Golden, and Briglia[7] studied dissociative ionization in CH_4 by measuring the cross section for production of ions with more than 0.25 eV of initial kinetic energy. Partial cross sections for CH_4 were measured by Adamczyk *et al.*,[8] Chatham *et al.*,[6] and Orient and Srivastava,[9] while partial cross sections for CD_4 were measured by Tarnovsky *et al.*[10] All previous partial cross section measurements were placed on an absolute scale by normalizing to a previously determined cross section for either methane or a rare gas.

This paper reports absolute partial cross sections for electron-impact ionization of CH_4 using an apparatus and technique that allow the individual cross sections to be determined absolutely through direct measurement of all the quantities needed for their evaluation. The results are obtained using a time-of-flight mass spectrometer in which the mass analyzed ions are detected with a position-sensitive detector whose output demonstrates that all product ions, regardless of their initial kinetic energy, are completely collected. The measured processes are the production of CH_4^+, CH_3^+, CH_2^+, CH^+, C^+, H_2^+, and H^+ for electron energies from threshold to 1000 eV.

II. APPARATUS AND EXPERIMENTAL METHOD

The apparatus shown in Fig. 1 consists of an electron gun, a time-of-flight mass spectrometer with position-sensitive detection, and an absolute pressure gauge (not shown). It has been described in detail previously.[11,12] Briefly, during a cross section measurement the entire vacuum chamber is filled with methane at a pressure of approximately 3×10^{-6} Torr. The electron gun produces 20 ns long pulses, each containing approximately 2500 electrons, at a repetition rate of 2.5 kHz. These pulses are directed through an interaction region, located between two plates maintained at ground potential, and are collected in a Faraday cup. Approximately 200 ns after each electron pulse, a 480 V/cm electric field is applied across the interaction region to drive any positive ions formed by electron impact

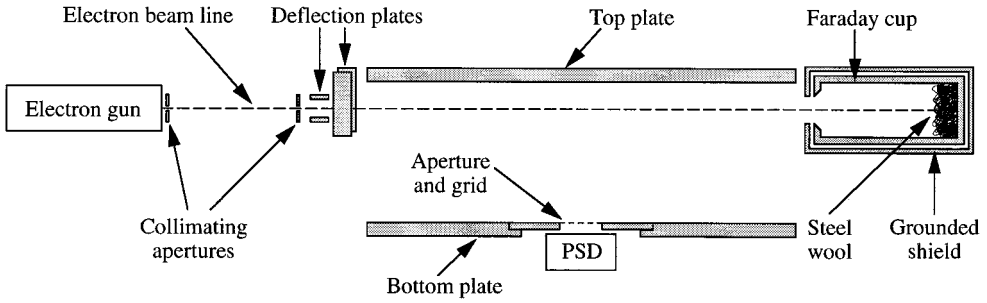

FIG. 1. Schematic diagram of the apparatus.

 0021-9606/97/106(11)/4430/6/$10.00

toward the bottom plate. This electric field is generated by applying a 3 kV pulse with a 55 ns rise time to the top plate. Some ions pass through a grid-covered aperture, of length 1.91 cm in the direction parallel to the electron beam, in the bottom plate. These ions are then accelerated to an energy of 5.4 keV and subsequently impact a position-sensitive detector (PSD), comprising a pair of 25 mm diameter microchannel plates and a resistive-encoded anode,[13] which records their arrival times and positions. The ion arrival times are used to identify their mass-to-charge ratios and the ion arrival positions are used to determine the effectiveness of product ion collection.

Under conditions in which very few of the incident electrons produce an ion, the partial cross section $\sigma(X)$ for production of ion species X is given by

$$\sigma(X)=\frac{N_i(X)}{N_e n l}, \tag{1}$$

where $N_i(X)$ is the number of X ions produced by a number N_e of electrons passing a distance l through a uniform methane target of number density n. Determination of an absolute cross section requires measurement of all four quantities on the right-hand side of Eq. (1) and has been previously described in detail.[11,12] Briefly, the number of electrons N_e is determined by collecting the electron beam in a Faraday cup and measuring the current with an electrometer operating in the charge collection mode. Measurement of $N_i(X)$ is accomplished by recording the time-of-flight spectrum, counting the number ions in an appropriate portion of the spectrum, and accounting for the detection efficiency for the combination of grid and PSD. This detection efficiency was determined to be $(37.8\pm0.2)\%$ and to be independent of ion species by repetitively directing an ion beam of appropriate species and energy alternately onto the PSD and into a second Faraday cup (not shown in Fig. 1). The effective path length l from which detected ions originate is accurately given by the 1.91 cm length of the aperture directly in front of the PSD.[12] The target number density n is obtained from measurements of the methane pressure using a capacitance diaphragm gauge.[14]

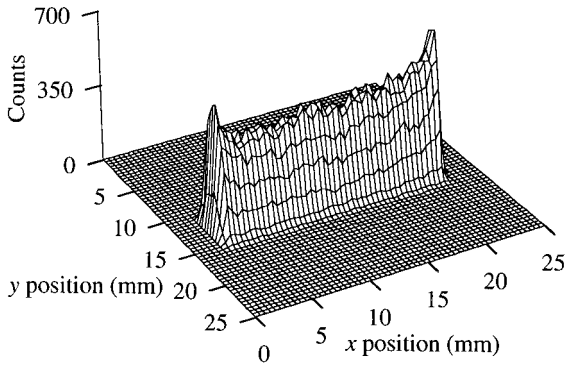

FIG. 2. Arrival position distribution for CH_4^+ ions produced by 200 eV electron impact on CH_4. The electron beam is parallel to the x direction.

The ion arrival position distribution of the CH_4^+ parent ions is shown in Fig. 2. These thermal energy ions impact the PSD in a narrow strip located directly beneath the electron beam. The position distribution is truncated at approximately 3 and 22 mm on the x axis due to the aperture immediately in front of the PSD. The enhanced signal seen at the ends of the position distribution is due to a slight focusing of the ions' trajectories that occurs after the ions have passed through the grid-covered aperture and during acceleration toward the PSD. This focusing, therefore, does not affect the effective path length from which detected ions originate being given by the length of the aperture.

Figure 3 shows a plot in which the ions' transverse arrival positions at the PSD (i.e., the displacement of ions perpendicular to the electron beam axis) have been combined with their flight times. This plot illustrates the mass resolution of the apparatus and gives qualitative information about the relative kinetic energies of the fragment ions. As can be

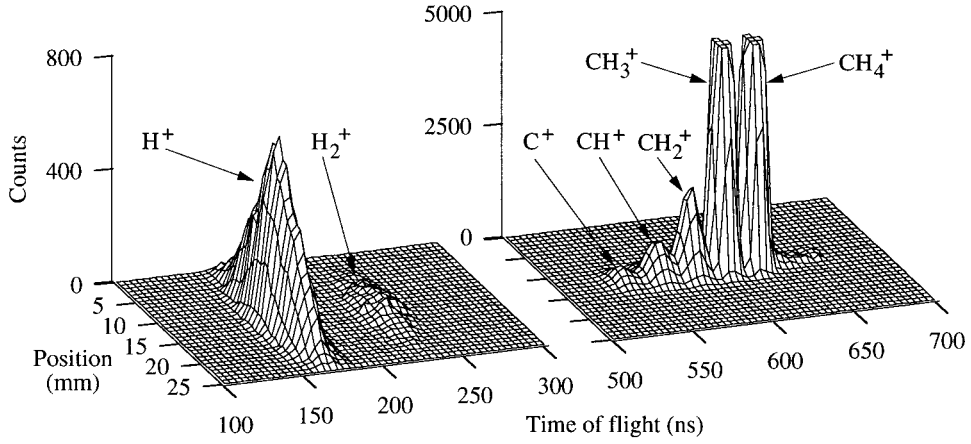

FIG. 3. Position and time-of-flight distribution produced by 200 eV electron impact on CH_4. Note that the tops of the CH_4^+ and CH_3^+ peaks have been cut off in order to provide more detail for the CH_2^+, CH^+, and C^+ peaks. The CH_4^+ and CH_3^+ peaks actually extend up to 14 000 and 12 500 counts, respectively.

TABLE I. Ion counting statistics and the relative and absolute uncertainties associated with the partial cross sections for CH_4. The ion counting statistics represent one standard deviation. The uncertainty for σ(Total) comes from an appropriately weighted sum of the uncertainties for the partial cross sections.

Cross section	Ion counting statistics (%)	Relative uncertainty (%)	Absoluteuncertainty at 200 eV (%)	Absolute uncertainty at all other energies (%)
$\sigma(CH_4^+)$	0.5	±2.0	±3.0	±3.5
$\sigma(CH_3^+)$	0.5	±2.0	±3.0	±3.5
$\sigma(CH_2^+)$	1.5	±4.0	±4.5	±5.0
$\sigma(CH^+)$	1.5	±4.0	±4.5	±5.0
$\sigma(C^+)$	3.5	±5.5	±6.0	±7.0
$\sigma(H_2^+)$	3.5	±4.0	±4.5	±6.0
$\sigma(H^+)$	1.0	±2.5	±3.5	±4.0
σ(Total)		±2.0	±3.0	±3.5

seen in the figure, the CH_x^+ ($x=0$–4) peaks are not completely resolved; however, it is estimated that the overlap of the peaks causes an error in cross section determination of not more than 0.5%, 0.5%, 3%, 3%, and 4% for the CH_4^+, CH_3^+, CH_2^+, CH^+, and C^+ cross sections, respectively. It can also be seen from Fig. 3 that no product ions, including H^+ which is the most energetic, have sufficient energy to reach beyond the edges of the PSD and thus escape detection. Without such information about ion arrival positions, it is virtually impossible to conclusively demonstrate complete ion collection.

III. CROSS SECTION DETERMINATION AND UNCERTAINTIES

Measurement of all the quantities on the right-hand side of Eq. (1) allows direct determination of absolute partial cross sections. Since pressure measurements using the capacitance diaphragm gauge needed for determination of the number density n are extremely time consuming, absolute measurement of the cross sections was made at an electron energy of 200 eV, and the relative shapes of the partial cross sections were determined by measuring the cross sections at

TABLE II. Present results for the partial cross sections of CH_4.

Energy (eV)	$\sigma(CH_4^+)$ (10^{-16} cm^2)	$\sigma(CH_3^+)$ (10^{-16} cm^2)	$\sigma(CH_2^+)$ (10^{-17} cm^2)	$\sigma(CH^+)$ (10^{-17} cm^2)	$\sigma(C^+)$ (10^{-18} cm^2)	$\sigma(H_2^+)$ (10^{-18} cm^2)	$\sigma(H^+)$ (10^{-17} cm^2)
15	0.197	0.038					
17.5	0.519	0.238	0.055				
20	0.892	0.512	0.169				
22.5	1.11	0.740	0.285				
25	1.29	0.923	0.559	0.045		0.065	0.074
30	1.46	1.12	1.41	0.314	0.323	0.113	0.308
35	1.51	1.19	2.18	0.800	1.51	0.646	0.750
40	1.55	1.22	2.65	1.19	2.93	1.60	1.39
45	1.61	1.27	2.97	1.43	3.67	2.38	2.10
50	1.63	1.29	3.07	1.50	4.49	2.86	2.66
60	1.65	1.33	3.18	1.69	5.09	3.41	3.50
70	1.66	1.35	3.21	1.78	5.71	3.73	4.03
80	1.64	1.34	3.23	1.75	6.08	3.85	4.34
90	1.62	1.33	3.14	1.78	6.02	3.92	4.52
100	1.60	1.31	3.12	1.70	6.00	3.89	4.53
110	1.56	1.29	3.05	1.66	6.01	3.78	4.52
125	1.52	1.25	2.90	1.55	5.81	3.62	4.33
150	1.44	1.18	2.70	1.40	5.30	3.37	3.99
175	1.37	1.13	2.48	1.28	4.78	2.97	3.69
200	1.31	1.08	2.34	1.16	4.43	2.64	3.42
250	1.17	0.970	2.01	0.978	3.53	2.23	2.78
300	1.07	0.886	1.78	0.839	3.05	1.95	2.39
400	0.918	0.742	1.40	0.634	2.10	1.42	1.83
500	0.799	0.655	1.19	0.518	1.66	1.14	1.47
600	0.703	0.574	1.02	0.428	1.40	1.01	1.23
700	0.636	0.518	0.892	0.372	1.22	0.852	1.03
800	0.562	0.463	0.796	0.322	0.951	0.735	0.888
900	0.524	0.427	0.725	0.299	0.908	0.598	0.787
1000	0.483	0.391	0.656	0.270	0.817	0.550	0.699

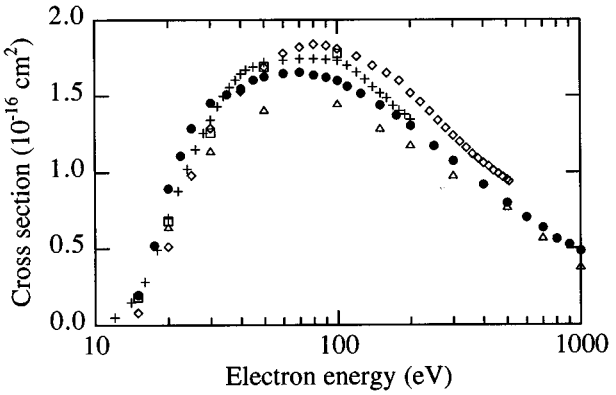

FIG. 4. Present CH_4^+ cross section (●) together with the results of Tarnovsky *et al.* (Ref. 10) (+); Orient and Srivastava (Ref. 9) (◇); Chatham *et al.* (Ref. 6) (□); and Adamczyk *et al.* (Ref. 8) (△).

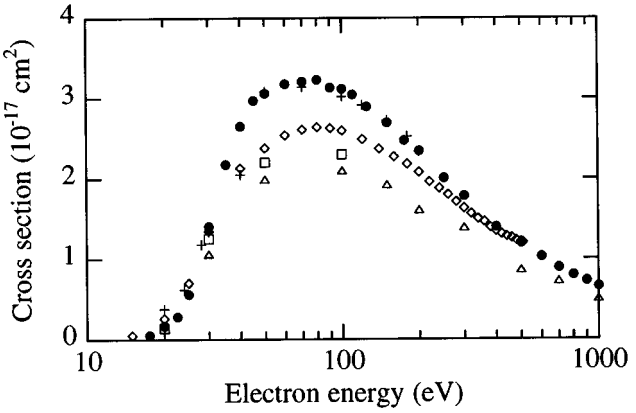

FIG. 6. Present CH_2^+ cross section (●) together with the results of Tarnovsky *et al.* (Ref. 10) (+); Orient and Srivastava (Ref. 9) (◇); Chatham *et al.* (Ref. 6) (□); and Adamczyk *et al.* (Ref. 8) (△).

various energies relative to the cross section at 200 eV. For methane pressures between 10^{-6} and 10^{-5} Torr, the measured cross sections were found to be invariant with respect to the pressure.

A detailed analysis of the experimental uncertainties has been given previously.[11] Table I gives the ion counting statistics and the relative and absolute uncertainties for all cross sections measured in this work. The relative uncertainties come from the ion counting statistics, the uncertainties (given in the previous section) due to incomplete separation of the CH_x^+ ($x=0$–4) peaks, and a ±0.5% uncertainty in the electron beam current measurement. The absolute uncertainties in the cross sections come from the ion counting statistics, the uncertainties (given in the previous section) due to incomplete separation of the CH_x^+ ($x=0$–4) peaks, a ±0.5% uncertainty associated with determination of the detection efficiency, a ±0.5% uncertainty in the electron beam current measurement, a ±0.5% uncertainty in the calibration of the electrometer used for the electron beam current measurement and PSD detection efficiency determination, a ±1% uncertainty in the target length, a ±2.5% statistical uncertainty and a ±1% calibration uncertainty in the pressure measurement with the capacitance diaphragm gauge, and a ±0.2% uncertainty in the temperature measurement needed for calculation of the number density. The energy of the electron beam was established to better than ±1 eV by observing the threshold for He^+ formation.

IV. RESULTS AND DISCUSSION

The measured partial cross sections for CH_4 are listed in Table II and are plotted in Figs. 4–10 together with previously published partial cross sections. The uncertainties in the present partial cross sections are given in Table I while the uncertainties in previous partial cross section measurements are typically ±15% or more. It is noteworthy that only the present partial cross sections are absolute, all other results were normalized using a previously determined cross section for either methane or a rare gas. Tarnovsky *et al.*[10] actually measured cross sections for electron-impact ionization of CD_4. It is meaningful to compare their CD_4 results to

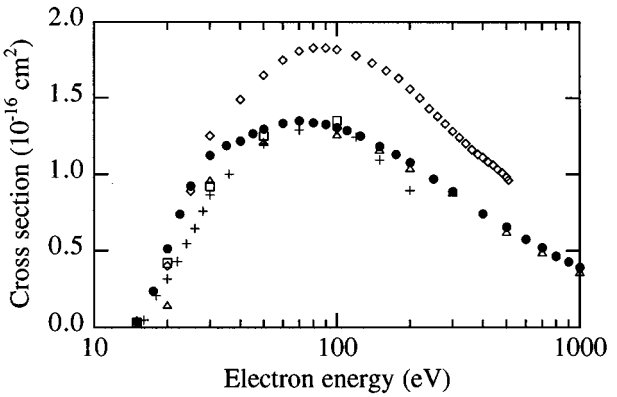

FIG. 5. Present CH_3^+ cross section (●) together with the results of Tarnovsky *et al.* (Ref. 10) (+); Orient and Srivastava (Ref. 9) (◇); Chatham *et al.* (Ref. 6) (□); and Adamczyk *et al.* (Ref. 8) (△).

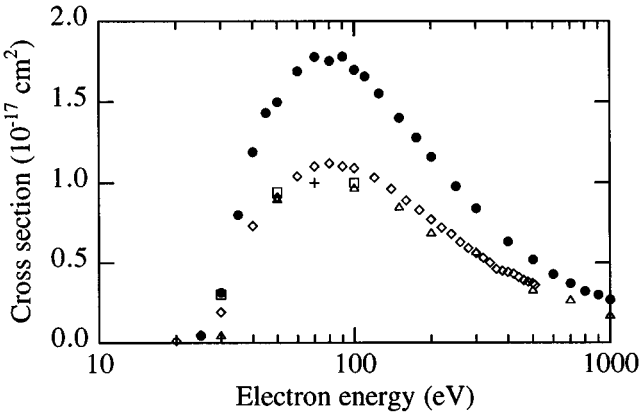

FIG. 7. Present CH^+ cross section (●) together with the results of Tarnovsky *et al.* (Ref. 10) (+); Orient and Srivastava (Ref. 9) (◇); Chatham *et al.* (Ref. 6) (□); and Adamczyk *et al.* (Ref. 8) (△).

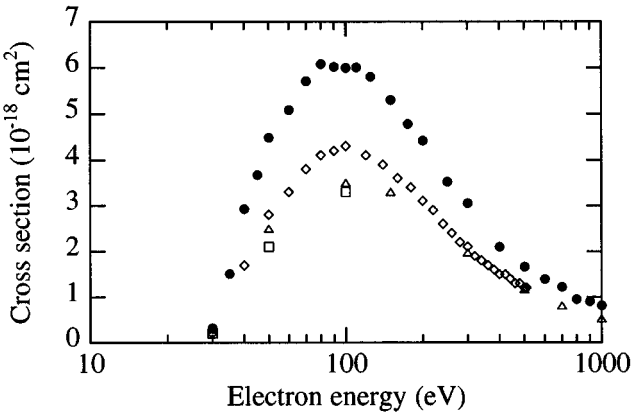

FIG. 8. Present C^+ cross section (●) together with the results of Orient and Srivastava (Ref. 9) (◇); Chatham *et al.* (Ref. 6) (□); and Adamczyk *et al.* (Ref. 8) (△).

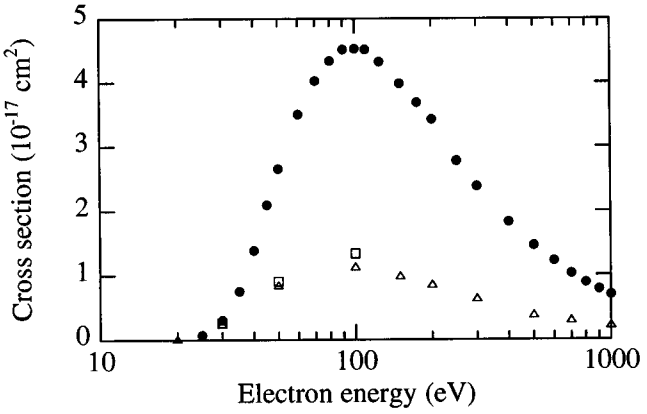

FIG. 10. Present H^+ cross section (●) together with the results of Chatham *et al.* (Ref. 6) (□) and Adamczyk *et al.* (Ref. 8) (△).

CH_4 measurements, however, since they noted that the partial cross sections for methane should be insensitive to isotopic effects.

All of the previous cross section measurements for CH_4^+ and CH_3^+ are in good agreement with the present results except for the CH_3^+ cross section of Orient and Srivastava.[9] For the CH_2^+ cross section, the results of Tarnovsky *et al.*[10] agree well with the present results while all other previous measurements tend to fall somewhat lower. For the remaining partial cross sections, all previous cross section measurements lie lower than the present results. The worst case is for the H^+ cross section in which the results of Chatham *et al.*[6] and Adamczyk *et al.*[8] are approximately a factor of 4 lower than the present results. These low measurements are attributed to incomplete collection of the fragment ions, particularly in the cases of H_2^+ and H^+ which can be seen in Fig. 3 to be the two most energetic fragment ions.

The total cross section, obtained as the sum of the partial cross sections, is shown in Fig. 11 together with previous direct absolute measurements of the total cross section. The results of Rapp and Englander-Golden[2] and Schram *et al.*[3] agree with the present results to within the combined uncertainties.

V. CONCLUSION

Measurements of the absolute partial cross section for electron-impact ionization of CH_4 have been presented. The apparatus geometry is of simple design embodying a short-path-length time-of-flight mass spectrometer and position-sensitive detection of the product ions which allows the complete collection of energetic fragment ions from dissociative ionization to be unequivocally demonstrated. Additionally, determination of the ions' detection efficiency and direct measurement of the methane gas pressure using a capacitance diaphragm gauge allows the cross sections to be measured absolutely. The present cross section measurements have been compared to previous results. Although good agreement is generally found for the CH_4^+ and CH_3^+ cross sections, almost all previous results for the remaining fragment ion cross sections are found to lie lower than the present measurements.

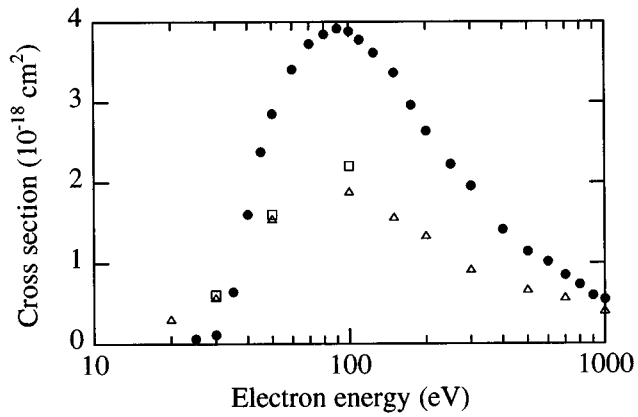

FIG. 9. Present H_2^+ cross section (●) together with the results of Chatham *et al.* (Ref. 6) (□) and Adamczyk *et al.* (Ref. 8) (△).

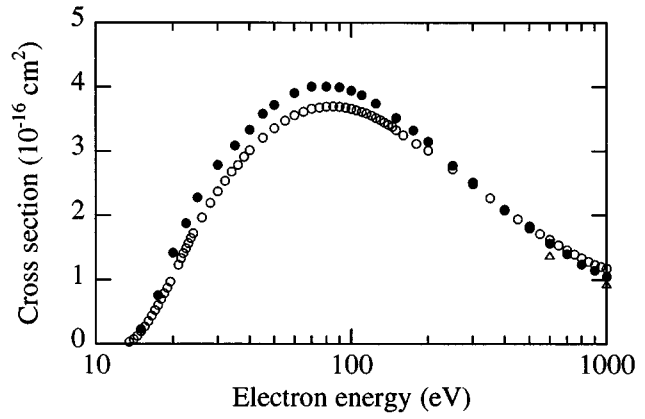

FIG. 11. Present CH_4 total cross section (●) together with the results of Schram *et al.* (Ref. 3) (△) and Rapp and Englander-Golden (Ref. 2) (○).

ACKNOWLEDGMENTS

We gratefully acknowledge support by the Atmospheric Sciences Section of the National Science Foundation, the National Aeronautics and Space Administration, and the Robert A. Welch Foundation.

[1] A. Ll. Hughes and E. Klein, Phys. Rev. **23**, 450 (1924).
[2] D. Rapp and P. Englander-Golden, J. Chem. Phys. **43**, 1464 (1965).
[3] B. L. Schram, M. J. van der Wiel, F. J. de Heer, and H. R. Moustafa, J. Chem. Phys. **44**, 49 (1966).
[4] B. A. Tozer, J. Electron. Control **4**, 149 (1958).
[5] H. F. Winters, J. Chem. Phys. **63**, 3462 (1975).
[6] H. Chatham, D. Hils, R. Robertson, and A. Gallagher, J. Chem. Phys. **81**, 1770 (1984).
[7] D. Rapp, P. Englander-Golden, and D. D. Briglia, J. Chem. Phys. **42**, 4081 (1965).
[8] B. Adamczyk, A. J. H. Boerboom, B. L. Schram, and J. Kistemaker, J. Chem. Phys. **44**, 4640 (1966).
[9] O. J. Orient and S. K. Srivastava, J. Phys. B **20**, 3923 (1987).
[10] V. Tarnovsky, A. Levin, H. Deutsch, and K. Becker, J. Phys. B **29**, 139 (1996).
[11] H. C. Straub, P. Renault, B. G. Lindsay, K. A. Smith, and R. F. Stebbings, Phys. Rev. A **52**, 1115 (1995).
[12] H. C. Straub, P. Renault, B. G. Lindsay, K. A. Smith, and R. F. Stebbings, Phys. Rev. A **54**, 2146 (1996); H. C. Straub, B. G. Lindsay, K. A. Smith, and R. F. Stebbings, J. Chem. Phys. **105**, 4015 (1996); B. G. Lindsay, H. C. Straub, K. A. Smith, and R. F. Stebbings, J. Geophys. Res. **101**, 21151 (1996).
[13] R. S. Gao, P. S. Gibner, J. H. Newman, K. A. Smith, and R. F. Stebbings, Rev. Sci. Instrum. **55**, 1756 (1984).
[14] H. C. Straub, P. Renault, B. G. Lindsay, K. A. Smith, and R. F. Stebbings, Rev. Sci. Instrum. **65**, 3279 (1994).